

2-Hydroxybenzamide as a Ligand. Complex Formation with Dioxouranium(VI), Aluminum(III), Neodymium(III), and Nickel(II) Ions

Emilia Furia* and Raffaella Porto†

Dipartimento di Chimica, Università della Calabria, via P. Bucci-87036 Arcavacata di Rende (CS), Italy

The complexation equilibria of 2-hydroxybenzamide (salicylamide, HL) with UO_2^{2+} , Al^{3+} , Nd^{3+} , and Ni^{2+} ions have been studied at 25 °C and in $1 \text{ mol}\cdot\text{dm}^{-3}$ NaClO_4 ionic medium by potentiometric measurements with a glass electrode. The concentration of ligand (C_L) was varied between $(1\cdot 10^{-3}$ and $15\cdot 10^{-3}) \text{ mol}\cdot\text{dm}^{-3}$, while the concentration of metal ions M^{z+} (C_M) ranged within $(0.5\cdot 10^{-3}$ and $10\cdot 10^{-3}) \text{ mol}\cdot\text{dm}^{-3}$. The ligand to metal concentration ratio was varied between 1 and 20. The hydrogen ion concentration was decreased stepwise to the incipient precipitation of a basic salt of each metal. The experimental data have been explained with the formation of the complexes: UO_2L^+ , UO_2L_2 , $\text{UO}_2(\text{HL})\text{L}^+$, $\text{UO}_2(\text{OH})\text{L}$, $(\text{UO}_2)_2(\text{OH})\text{L}_2^+$, $(\text{UO}_2)_2(\text{OH})_2^{2+}$, and $(\text{UO}_2)_3(\text{OH})_5^+$; AlL^{2+} , AlL_2^+ , $\text{Al}(\text{OH})\text{L}_2$, AlOH^{2+} , $\text{Al}(\text{OH})_2^+$, and $\text{Al}_3(\text{OH})_4^{5+}$; NdL^{2+} , NdL_2^+ , NdOH^{2+} , and $\text{Nd}_2\text{OH}_2^{4+}$; and NiL^+ , $\text{Ni}(\text{OH})\text{L}$, and NiOH^+ . Equilibrium formation constants are given for the investigated ionic media as well as for the infinite dilution reference state, evaluated by the specific ion interaction theory (SIT).

Introduction

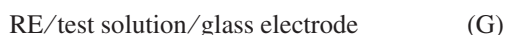
In recent years, we have been interested in a systematic study concerning the complexation of metal ions with salicylic acid and its derivatives. Because of its high solubility in aqueous solutions, hydrogen-salicylate sodium salt can be used over a wide range of concentrations. On the contrary, its derivatives present low solubility in water, and as a matter of fact, research in the literature¹ shows that data are scanty and measurements are chiefly carried out in nonaqueous solvents.

The purpose of this work is to study the complexing power of salicylamide toward metals, already investigated with salicylic acid,² to evaluate differences and similarities in behavior.

Method

The complexation equilibria have been studied, at 25 °C and in $1 \text{ mol}\cdot\text{dm}^{-3}$ NaClO_4 , by measuring with a glass electrode the competition of the salicylamide, HL, for the metal and H^+ ions.

The potentiometric measurements, performed as titrations, were made with cell (G)



where RE, reference electrode, = $\text{Ag}/\text{AgCl}/0.01 \text{ mol}\cdot\text{dm}^{-3}$ AgClO_4 , $0.99 \text{ mol}\cdot\text{dm}^{-3}$ $\text{NaClO}_4/1 \text{ mol}\cdot\text{dm}^{-3}$ NaClO_4 and test solution = $C_M \text{ mol}\cdot\text{dm}^{-3}$ $\text{M}(\text{ClO}_4)_z$, $C_L \text{ mol}\cdot\text{dm}^{-3}$ HL, $C_A \text{ mol}\cdot\text{dm}^{-3}$ HClO_4 , $C_B \text{ mol}\cdot\text{dm}^{-3}$ NaOH , $(1 - zC_M - C_A - C_B) \text{ mol}\cdot\text{dm}^{-3}$ NaClO_4 .

The metal concentration, C_M , ranged from $(0.5\cdot 10^{-3}$ to $10\cdot 10^{-3}) \text{ mol}\cdot\text{dm}^{-3}$, and the ligand concentration, C_L , was varied between $(1\cdot 10^{-3}$ and $15\cdot 10^{-3}) \text{ mol}\cdot\text{dm}^{-3}$ and $1 \leq C_L/C_M \leq 20$. The higher C_L value is imposed by the limited solubility of the ligand. The hydrogen ion concentration was varied from $10^{-2} \text{ mol}\cdot\text{dm}^{-3}$ to incipient precipitation of a basic

salt for each metal which depends on the particular metal ion and the ratio ligand/metal.

Since the effects of composition changes on activity coefficients can be considered negligible, the EMF of cell (G) can be written, in millivolts, at the temperature of 25 °C, as 1

$$E = E^\circ + 59.16 \log[\text{H}^+] + E_j \quad (1)$$

where E° is constant in each series of measurements and E_j is the liquid junction potential which is a function of $[\text{H}^+]$ only.³ In a previous study, we have found⁴ $E_j = -58[\text{H}^+]$ in $1 \text{ mol}\cdot\text{dm}^{-3}$ NaClO_4 .

Each titration was divided in two parts. In the first part, E° was determined in the absence of M^{z+} ions. In the second part, the acidity was varied by different methods according to the nature of the equilibrium investigated. Thus, $[\text{H}^+]$ was decreased stepwise by coulometric generation of OH^- ions with the circuit (C) described in Reagents and Analysis, when the equilibria involved the Al^{3+} and Nd^{3+} ions. For the investigation of uranyl and nickel complexes, alkalification was achieved by adding NaOH .

The primary C_M , C_L , C_A , C_B , and $[\text{H}^+]$ data form the basis of the treatment to obtain the equilibrium constants.

Experimental Section

Reagents and Analysis. Aluminum(III) perchlorate was prepared and standardized as reported by Ciavatta and Iuliano.⁵

Nickel(II) perchlorate was prepared and standardized as reported by Biedermann and Ferri.⁶

Neodymium(III) and dioxouranium(VI) perchlorates, perchloric acid, and sodium perchlorate stock solutions were prepared and standardized as described previously.²

Sodium hydroxide stock solutions were prepared by different methods according to the nature of the metal ion investigated. When the metal cation, such as Al^{3+} and Nd^{3+} , is not reducible at the cathode of an electrolyte cell, an exact amount of sodium hydroxide was added by coulometric generation of OH^- ions with circuit (C)

* Corresponding author. E-mail: e.furia@unical.it. Tel.: +39-0984-492056. Fax: +39 -0984-492044.

† Professor Raffaella Porto passed away on May 18th, 2008.



where AE, auxiliary electrode, = 1 M NaClO₄/0.1 M NaCl, 0.9 M NaClO₄/Hg₂Cl₂/Hg.

Assuming that at the cathode the only reactions that occur are $\text{H}^+ + \text{e}^- \rightarrow 1/2\text{H}_2$ and $\text{H}_2\text{O} + \text{e}^- \rightarrow 1/2\text{H}_2 + \text{OH}^-$, then in the test solution, of a given volume $V \text{ dm}^3$, $C_B = \mu\text{F}10^{-6}/V \text{ mol}\cdot\text{dm}^{-3}$, where μF stands for the microfaradays passed through the cell.

In the investigation of nickel and uranyl complexes, where the generation did not proceed with 100 % current efficiency, sodium hydroxide titrant solutions were obtained by dilution of a saturated solution filtered on a Gooch crucible (G4) in nitrogen atmosphere. The hydroxide concentration was determined by titration with standardized HClO₄ using methyl-red as a visual indicator. The results agreed to within 0.1 %.

Salicylamide (Aldrich p.a.) was used without further purification. It was kept in a desiccator over silica gel.

All solutions were prepared with twice distilled water.

Apparatus. The cell arrangement was similar to the one described by Forsling et al.⁷

Ag/AgCl electrodes were prepared according to Brown.⁸

Glass electrodes, manufactured by Metrohm, were of the 6.0133.100 type. They acquired a constant potential within 10 min after the addition of the reagents and remained unchanged to within $\pm 0.1 \text{ mV}$ for several hours.

The titrations were carried out with a programmable computer controlled data acquisition switch unit 34970 A supplied by Hewlett and Packard.

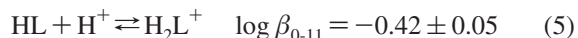
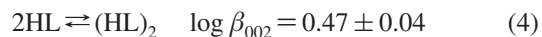
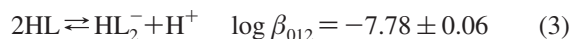
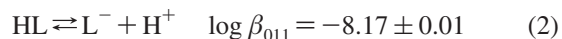
The EMF values were measured with a precision of $\pm 10^{-5} \text{ V}$ using an OPA 111 low-noise precision DIFET operational amplifier. A slow stream of nitrogen gas was passed through four bottles containing $1 \text{ mol}\cdot\text{dm}^{-3} \text{ NaOH}$, $1 \text{ mol}\cdot\text{dm}^{-3} \text{ H}_2\text{SO}_4$, twice distilled water, and $1 \text{ mol}\cdot\text{dm}^{-3} \text{ NaClO}_4$, respectively, and then into the test solutions through the gas inlet tube.

During the EMF measurements, the cell assembly was placed in a thermostat kept at $(25.0 \pm 0.1) \text{ }^\circ\text{C}$.

Treatment of the Data and Results

On the Salicylamide Acidic Equilibria. The acid-base properties of the ligand have been studied at 25 °C and in NaClO₄ media for ionic strengths ranging from (0.5 to 3) $\text{mol}\cdot\text{dm}^{-3}$ using EMF as well as solubility measurements.

The data will be described in detail in a forthcoming paper. The results, relative to $1 \text{ mol}\cdot\text{dm}^{-3} \text{ NaClO}_4$, are concisely reported here. A comparison with literature data is not possible since they derive from measurements carried out in nonaqueous solvents because of the low solubility of salicylamide.



The uncertainties represent 3σ . Equilibria 2, 3, and 4 were obtained from potentiometric titrations with cell G where $C_M = 0$. Information on equilibrium 5 has been obtained in the acidic range ($[\text{H}^+] > 0.1 \text{ mol}\cdot\text{dm}^{-3}$) from solubility measurements. Starting solutions contained a NaClO₄ and HClO₄ mixture, and the ionic strength was $1 \text{ mol}\cdot\text{dm}^{-3}$ and then an excess of pure salicylamide was added. Test solutions were analyzed by spectrophotometric measurements in the ultraviolet region ($\lambda = 299 \text{ nm}$) after suitable dilution with twice distilled

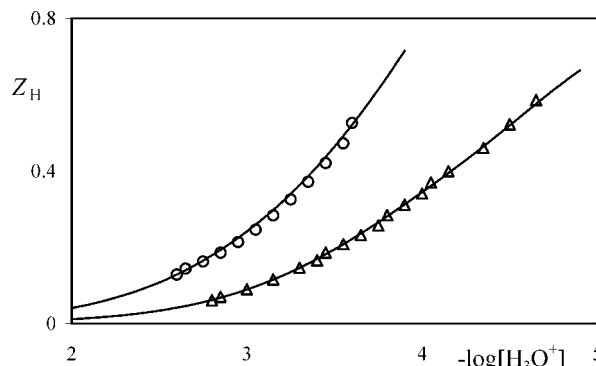


Figure 1. Uranyl-HL system Z_H in function of $-\log[\text{H}_3\text{O}^+]$. For clarity, only two of four titrations are reported in the figure. The symbols refer to $C_M 10^3 \text{ mol}\cdot\text{dm}^{-3}$, $C_L 10^3 \text{ mol}\cdot\text{dm}^{-3}$: triangles, (3, 6); circles, (10, 10). The curves have been calculated by assuming the constants given in Table 5.

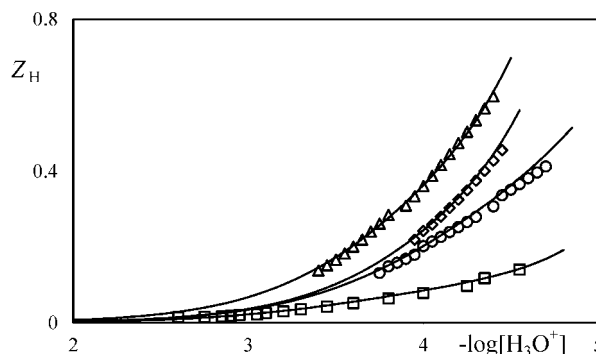
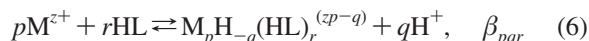


Figure 2. Al(III)-HL system Z_H in function of $-\log[\text{H}_3\text{O}^+]$. For clarity, only four of nine titrations are reported. The symbols refer to $C_M 10^3 \text{ mol}\cdot\text{dm}^{-3}$, $C_L 10^3 \text{ mol}\cdot\text{dm}^{-3}$: diamond, (1, 1); triangles, (2, 2); circles, (1, 2); squares, (0.5, 10). The curves have been calculated by assuming the constants given in Table 6.

water. The absorbance increase resulting from an increase of acid confirms the existence of equilibrium 5.

Data Analysis: Calculation of β_{pqr} Values. The general equilibrium can be written, schematically, for all the four systems as 6



For a visualization of the equilibria the function Z_H , the average number of H_3O^+ ions split off per HL was calculated as a function of $-\log[\text{H}_3\text{O}^+]$ from the primary data

$$Z_H = ([\text{H}_3\text{O}^+] - K_w[\text{H}_3\text{O}^+]^{-1} - C_A + C_B)/C_L \quad (7)$$

where $K_w = 10^{-13.74}$ is from Baes and Mesmer.⁹ In Figures 1, 2, 3, and 4 are reported the experimental function Z_H for the different systems. These figures do not contain all the data, but in Tables 1 to 4, there is a summary of the relevant data taken in all titrations for each of the metals. The limiting Z_H ($-\log[\text{H}_3\text{O}^+] \rightarrow 0$), represented by the dashed curves in Figures 3 and 4, is seen to fall not very far from the data relative to the Nd^{3+} and Ni^{2+} systems. This is an indication that these cations form complexes of low stability. On the other hand, data relative to Al(III) and U(VI), Figures 1 and 2, are displaced by more than four log in units $[\text{H}_3\text{O}^+]$ from the limiting curve (not drawn in the figures). Therefore, the Al(III) and U(VI) complexes are of larger stability.

The most probable p , q , and r values and the corresponding constants β_{pqr} were computed by a numerical approach based on the least-squares procedure using the program SUPER-

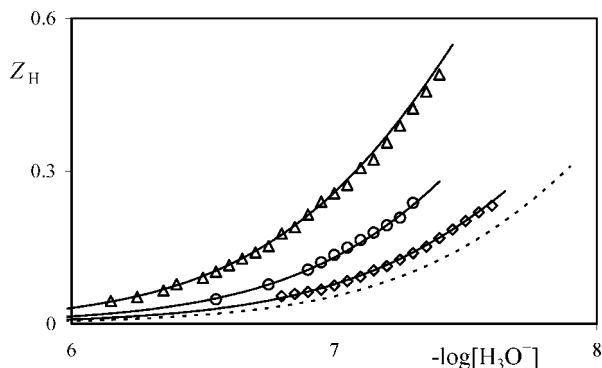


Figure 3. Nd(III)–HL system Z_H in function of $-\log[\text{H}_3\text{O}^+]$. For clarity, only three of six titrations are reported. The symbols refer to C_M 10^3 mol·dm⁻³, C_L 10^3 mol·dm⁻³: diamond, (0.5, 10); circles, (1.5, 3); triangles, (5, 10). The curves have been calculated by assuming the constants given in Table 7. The dashed curve represents the curve in the absence of metal.

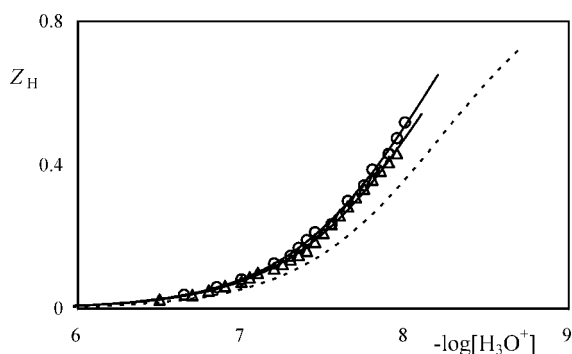


Figure 4. Ni(II)–HL system Z_H in function of $-\log[\text{H}_3\text{O}^+]$. For clarity, only two of four titrations are reported. The symbols refer to C_M 10^3 mol·dm⁻³, C_L 10^3 mol·dm⁻³: circles, (5, 5); triangles, (5, 10). The curves have been calculated by assuming the constants given in Table 8. The dashed curve represents the curve in the absence of metal.

Table 1. Summary of the Relevant Data Taken in Four Titrations for the System UO_2^{2+} –Salicylamide

C_M	C_L	pH range	Z_H range
$5 \cdot 10^{-3}$	$15 \cdot 10^{-3}$	2.4 to 2.9	$6.5 \cdot 10^{-2}$ to 0.12
$10 \cdot 10^{-3}$	$10 \cdot 10^{-3}$	2.5 to 3.3	0.12 to 0.37
$3 \cdot 10^{-3}$	$3 \cdot 10^{-3}$	3.3 to 5.1	0.12 to 1.34
$3 \cdot 10^{-3}$	$6 \cdot 10^{-3}$	2.8 to 4.7	$6.1 \cdot 10^{-2}$ to 0.58

Table 2. Summary of the Relevant Data Taken in Nine Titrations for the System Al^{3+} –Salicylamide

C_M	C_L	pH range	Z_H range
$0.5 \cdot 10^{-3}$	$10 \cdot 10^{-3}$	3.8 to 5.3	$4.3 \cdot 10^{-2}$ to 0.1
$1 \cdot 10^{-3}$	$10 \cdot 10^{-3}$	2.5 to 4.3	$1.5 \cdot 10^{-2}$ to 0.12
$1 \cdot 10^{-3}$	$1 \cdot 10^{-3}$	4.0 to 4.4	0.25 to 0.45
$1 \cdot 10^{-3}$	$2 \cdot 10^{-3}$	3.7 to 4.6	0.13 to 0.41
$1 \cdot 10^{-3}$	$3 \cdot 10^{-3}$	3.6 to 4.8	0.12 to 0.35
$2 \cdot 10^{-3}$	$6 \cdot 10^{-3}$	3.4 to 4.5	0.12 to 0.37
$2 \cdot 10^{-3}$	$2 \cdot 10^{-3}$	3.7 to 4.3	0.24 to 0.60
$10 \cdot 10^{-3}$	$10 \cdot 10^{-3}$	3.1 to 4.1	0.29 to 0.77
$5 \cdot 10^{-3}$	$10 \cdot 10^{-3}$	3.1 to 4.4	0.16 to 0.53

QUAD.¹⁰ The minimum of the function $U = \sum w_i (E_{\text{exp}} - E_{\text{calc}})$ was sought, where w_i represents a statistical weight assigned to each point. Calculations of the χ -square statistic have been considered to test the fit between a theoretical frequency distribution and a frequency distribution of observed data. In the numerical treatment, the equilibrium constants concerning the species formed according to equilibria (2 to 5) have been maintained invariant. The single systems were treated separately.

System UO_2^{2+} –Salicylamide. The data comprise 4 titrations with 72 data points. A summary of the relevant data taken in

Table 3. Summary of the Relevant Data Taken in Six Titrations for the System Nd^{3+} –Salicylamide

C_M	C_L	pH range	Z_H range
$0.5 \cdot 10^{-3}$	$10 \cdot 10^{-3}$	6.8 to 8.6	$5.0 \cdot 10^{-2}$ to 0.33
$0.6 \cdot 10^{-3}$	$15 \cdot 10^{-3}$	6.4 to 7.2	$3.3 \cdot 10^{-2}$ to 0.11
$5 \cdot 10^{-3}$	$5 \cdot 10^{-3}$	6.5 to 7.2	0.10 to 0.43
$1.5 \cdot 10^{-3}$	$3 \cdot 10^{-3}$	6.7 to 7.3	$4.8 \cdot 10^{-2}$ to 0.25
$5 \cdot 10^{-3}$	$10 \cdot 10^{-3}$	6.8 to 7.3	0.15 to 0.49
$2.8 \cdot 10^{-3}$	$2.8 \cdot 10^{-3}$	6.6 to 7.0	$5.5 \cdot 10^{-2}$ to 0.20

Table 4. Summary of the Relevant Data Taken in Four Titrations for the System Ni^{2+} –Salicylamide

C_M	C_L	pH range	Z_H range
$5 \cdot 10^{-3}$	$10 \cdot 10^{-3}$	7.1 to 7.8	0.1 to 0.43
$5 \cdot 10^{-3}$	$15 \cdot 10^{-3}$	6.5 to 8.0	$6.6 \cdot 10^{-2}$ to 0.48
$5 \cdot 10^{-3}$	$5 \cdot 10^{-3}$	7.3 to 7.9	0.17 to 0.52
$30 \cdot 10^{-3}$	$15 \cdot 10^{-3}$	6.6 to 7.3	0.10 to 0.46

Table 5. Best Set of $\log \beta_{pqr}$ (σ) for the System Dioxouranium(VI)–Salicylamide

species	model 1	model 2	model 3	model 4
UO_2L^+	−1.60 (5)	−1.36 (1)	−1.51 (2)	−1.52 (1)
UO_2L_2		−4.05 (4)	−4.19 (5)	−4.18 (4)
$\text{UO}_2(\text{HL})\text{L}^+$			+0.35 (3)	+0.37 (3)
$\text{UO}_2(\text{OH})\text{L}$			−6.9 (1)	−6.9 (1)
$(\text{UO}_2)_2(\text{OH})\text{L}_2^+$				−5.9 (1)
$(\text{UO}_2)_2(\text{OH})_2^{2+}$	−5.4 (1)	−6.3 (1)	−5.91 (3)	−5.93 (3)
$(\text{UO}_2)_3(\text{OH})_5^+$	−15.6 (1)	−16.20 (5)	−16.33 (3)	−16.38 (3)
σ , mV	3.71	1.02	0.40	0.34
χ^2	9.31	15.03	8.17	6.34
U	$8.81 \cdot 10^2$	$6.55 \cdot 10^1$	9.72	6.85

Table 6. Best Set of $-\log \beta_{pqr}$ (σ) for the System Al(III)–Salicylamide

species	model 1	model 2	model 3	model 4
AlL^{2+}	1.388 (3)	1.387 (3)	1.387 (3)	1.422 (2)
AlL_2^+	4.09 (1)	4.09 (1)	4.10 (1)	4.162 (4)
AlL_3		8.6 (1)	rejected	
$\text{Al}(\text{OH})\text{L}_2$			10.6 (1)	10.80 (3)
AlOH^{2+}				5.91 (6)
AlOH_2^+				10.51 (4)
$\text{Al}_3\text{OH}_4^{5+}$				12.94 (3)
σ , mV	1.19	1.13	1.12	0.26
χ^2	74.83	79.92	77.25	23.42
U	$2.60 \cdot 10^2$	$2.34 \cdot 10^2$	$2.29 \cdot 10^2$	$1.25 \cdot 10^1$

Table 7. Best Set of $-\log \beta_{pqr}$ (σ) for the System Nd(III)–Salicylamide

species	model 1	model 2	model 3
NdL^{2+}	5.22 ± 0.01	5.296 ± 0.006	5.360 ± 0.009
NdL_2^+	11.08 ± 0.06	11.21 ± 0.03	11.17 ± 0.02
NdOH^{2+}			8.513 ± 0.05
$\text{Nd}_2\text{OH}_2^{4+}$		13.31 ± 0.02	13.45 ± 0.03
σ , mV	1.23	0.46	0.36
χ^2	96.38	45.7	17.42
U	$1.81 \cdot 10^2$	$2.51 \cdot 10^1$	$1.47 \cdot 10^1$

all titrations is reported in Table 1. The numerical treatment started assuming the presence of only UO_2L^+ and the dominant hydrolysis products of the dioxouranium ion, i.e., $(\text{UO}_2)_2(\text{OH})_2^{2+}$ and $(\text{UO}_2)_3(\text{OH})_5^+$ (model 1), but the standard deviation is higher than the experimental uncertainty.

Various models were tested by adding one single species. The best agreement was obtained with UO_2L_2 (model 2). A further improvement was reached including in the previous model the species $\text{UO}_2(\text{HL})\text{L}^+$ and $\text{UO}_2(\text{OH})\text{L}$ (model 3); on the other hand, on adding the polynuclear complex $(\text{UO}_2)_2(\text{OH})\text{L}_2^+$ (model 4), the fit is significantly improved. The various steps of calculations are illustrated in Table 5. The minor species $\text{UO}_2(\text{HL})\text{L}^+$, $\text{UO}_2(\text{OH})\text{L}$, and $(\text{UO}_2)_2(\text{OH})\text{L}_2^+$ reach, in particular experimental conditions, percentages that are not

Table 8. Best Set of $-\log \beta_{pqr} (\sigma)$ for the System Ni(II)–Salicylamide

species	model 1	model 2	model 3
NiL ⁺	6.09 ± 0.02	6.32 ± 0.02	6.31 ± 0.02
Ni(OH)L			14.80 ± 0.04
NiOH ⁺		8.81 ± 0.03	9.02 ± 0.04
σ , mV	1.93	0.65	0.36
χ^2	2.80	9.20	31.60
U	1.84 · 10 ²	2.05 · 10 ¹	6.09

negligible as can be seen in the distribution diagram reported in Figure 5. This gives some confidence to the presence of such species.

The hydrolysis of the uranyl ion has been studied extensively.¹¹ Hydrolysis constants for the dominant uranyl hydrolysis species, (2, 2, 0) and (3, 5, 0), obtained in this work are in excellent agreement with those determined in 1 M NaClO₄ and at 25 °C by Rush and Johnson¹² as well as with those obtained at different ionic strengths by Brown.¹³

System Al(III)–Salicylamide. The data comprise nine titrations with 192 data points. A summary of the relevant data taken in all titrations is reported in Table 2. Model 1 including only the species AlL²⁺ and AlL₂⁺ yields a fit that is only slightly improved by adding AlL₃ (model 2). However, this species is rejected when Al(OH)L₂ is assumed (model 3). No other species containing the ligand produces a significant lowering of the function U . On the other hand, on adding the hydrolytic complexes AlOH²⁺, Al(OH)₂⁺, and Al₃(OH)₄⁵⁺ (model 4), the fit is significantly improved indicating that these species are formed in appreciable amounts in our solutions. The polynuclear hydrolysis species (13, 32, 0) is known⁹ to form in high concentrations in Al systems. However, it has not been considered in the numerical treatment because our experimental conditions are not favorable to its formation. As no other species lowered the minimum, model 4 was assumed as the best describing the data, also in consideration that the standard deviation (σ) is comparable with the experimental uncertainty. The various steps of calculations are illustrated in Table 6.

Using the values of the constants reported in Table 6 (model 4), distribution diagrams were constructed (Figure 6). As can be seen in Figure 6a when the analytical concentrations of ligand are greater than those of the metal, e.g. $C_L = 10 \cdot 10^{-3} \text{ mol} \cdot \text{dm}^{-3}$ and $C_M = 0.5 \cdot 10^{-3} \text{ mol} \cdot \text{dm}^{-3}$, AlL²⁺ and AlL₂⁺ are the predominant species. When the analytical concentrations of ligand and metal are comparable (Figure 6b) in addition to the metal–ligand complexes AlL²⁺ and AlL₂⁺, also the hydrolytic species Al₃(OH)₄⁵⁺ reaches a significant percentage.

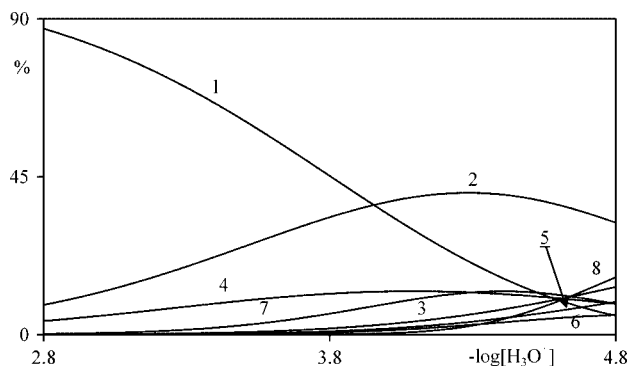


Figure 5. Distribution of the U(VI) species in $C_L = 6 \cdot 10^{-3} \text{ mol} \cdot \text{dm}^{-3}$, $C_M = 3 \cdot 10^{-3} \text{ mol} \cdot \text{dm}^{-3}$. 1, UO₂²⁺; 2, UO₂L⁺; 3, UO₂L₂; 4, UO₂(HL)L⁺; 5, UO₂(OH)L; 6, (UO₂)₂(OH)L₂⁺; 7, (UO₂)₂(OH)₂2⁺; 8, (UO₂)₃(OH)₅⁺.

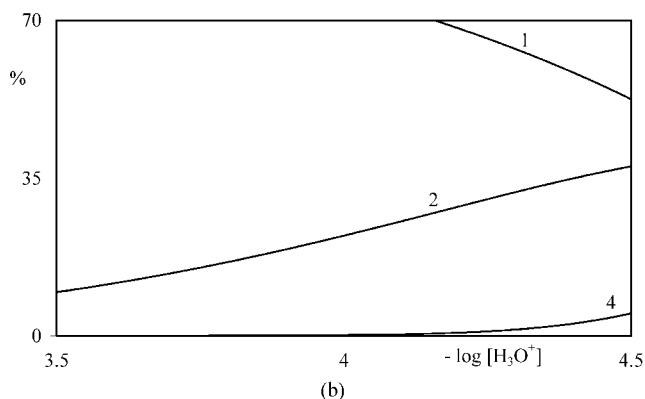
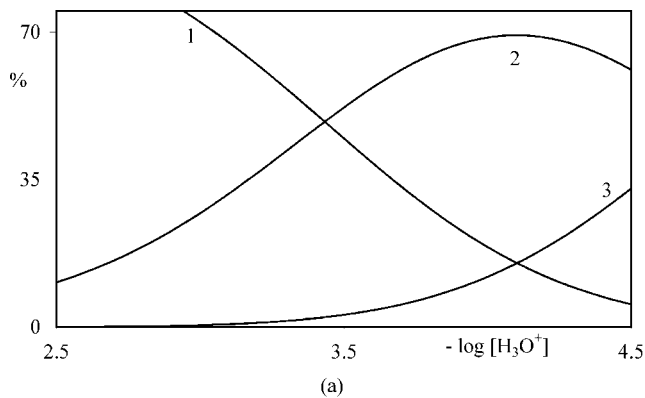


Figure 6. Distribution of Al(III) species for (a) $C_L = 10 \cdot 10^{-3} \text{ mol} \cdot \text{dm}^{-3}$, $C_M = 0.5 \cdot 10^{-3} \text{ mol} \cdot \text{dm}^{-3}$ and (b) $C_L = 1 \cdot 10^{-3} \text{ mol} \cdot \text{dm}^{-3}$, $C_M = 1 \cdot 10^{-3} \text{ mol} \cdot \text{dm}^{-3}$. 1, Al³⁺; 2, AlL²⁺; 3, AlL₂⁺; 4, Al₃(OH)₄⁵⁺.

In our experimental conditions, no other minor species attain significant percentages. For this reason, we have attempted a new model in the absence of these complexes. We have obtained a higher standard deviation and function U ($\sigma = 0.54 \text{ mV}$ and $U = 5.33 \cdot 10^1$) so that the presence of Al(OH)L₂, AlOH²⁺, and Al(OH)₂⁺ was assumed probable.

The hydrolysis constant for the aluminum hydrolysis species (3, 4, 0) obtained in this work is in good agreement with that determined in 1 M NaClO₄ and at 25 °C by Aveston.¹⁴ On the other hand, hydrolysis constants for the mononuclear aluminum hydrolysis species (1, 1, 0) and (1, 2, 0) obtained in this work differ significantly from those determined in the same ionic media.^{15,16} These differences may be due to the low percentage of these species in our experimental conditions, as evident in the distribution diagrams (Figure 6).

System Nd(III)–Salicylamide. The experimental data consist of 124 data points collected in 6 titrations. A summary of the relevant data taken in all titrations is reported in Table 3.

As the starting model, we considered the presence of the species NdL²⁺ and NdL₂⁺ (model 1). No other species involving metal and ligand ions were retained, thus the hydrolytic products were allowed to vary systematically. By adding the species Nd₂(OH)₂⁴⁺, the function U decreased by more than 80 % (model 2). A further improvement was reached with the introduction of the minor species NdOH²⁺ (model 3). The standard deviation marginally exceeds the experimental error since only a small amount of complexation takes place. Results are reported in Table 7.

The refined equilibrium constants are used to represent the distribution of neodymium in the different species (Figure 7). The predominant species in the overall pH range is NdL²⁺ which reaches percentages close to 25 %, but also the minor species

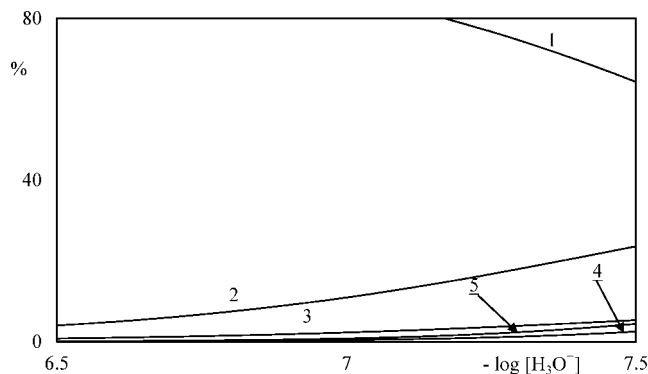


Figure 7. Distribution diagram of Nd(III) species for $C_L = 3 \cdot 10^{-3} \text{ mol} \cdot \text{dm}^{-3}$, $C_M = 1.5 \cdot 10^{-3} \text{ mol} \cdot \text{dm}^{-3}$. 1, Nd^{3+} ; 2, NdL^{2+} ; 3, NdL_2^+ ; 4, NdOH^{2+} ; 5, $\text{Nd}_2(\text{OH})_2^{4+}$.

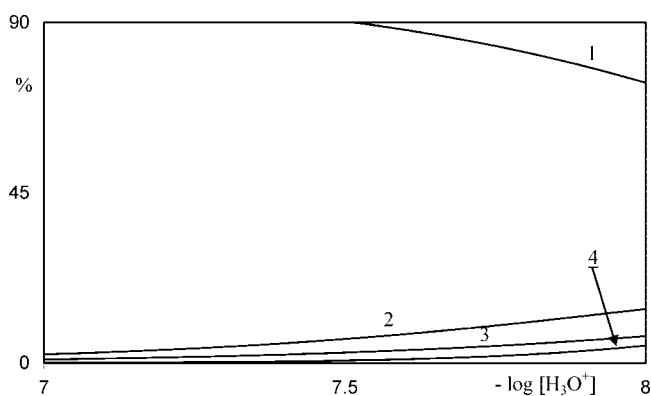


Figure 8. Distribution of Ni(II) species for $C_L = 5 \cdot 10^{-3} \text{ mol} \cdot \text{dm}^{-3}$, $C_M = 5 \cdot 10^{-3} \text{ mol} \cdot \text{dm}^{-3}$. 1, Ni^{2+} ; 2, NiL^+ ; 3, $\text{Ni}(\text{OH})\text{L}$; 4, NiOH^+ .

NdL_2^+ , NdOH^{2+} , and $\text{Nd}_2(\text{OH})_2^{4+}$ attain appreciable concentrations in our experimental conditions.

Literature data reporting neodymium hydrolysis are scanty. However, hydrolysis constants for the neodymium hydrolysis species, (1, 1, 0) and (2, 2, 0), obtained in this work are in good agreement with those reported by Baes and Mesmer.⁹

System Ni^{2+} –Salicylamide. The data comprise 4 titrations with 70 data points. A summary of the relevant data taken in all titrations is reported in Table 4. Model 1 considers only the presence of NiL^+ , but the standard deviation was considerably high. The introduction of the mononuclear hydrolytic product NiOH^+ (model 2) lowers σ about three times. A still better agreement was achieved by adding also $\text{Ni}(\text{OH})\text{L}$. On adding other species, the minimum could not be lowered so that model 3 was assumed as the best describing the data. The various steps of calculations are illustrated in Table 8. To visualize the amounts of the different species, the distribution diagram, given in Figure 8, was constructed. When the analytical concentrations of ligand and metal are comparable, in addition to the metal–ligand complexes also the hydrolytic species $\text{Ni}(\text{OH})^+$ reaches a significant percentage.

The hydrolysis of the nickel ion has been studied extensively.¹⁷ The hydrolysis constant for the nickel hydrolysis species (1, 1, 0) obtained in this work differs from that determined by Bolzan et al.¹⁸ in the same ionic media. This disagreement may be due to low percentage of this species in our experimental conditions, as evident in the distribution diagram (Figure 8).

Extrapolation to Infinite Dilution Reference State

Some practical applications require knowledge of the constants at the infinite dilution reference state. The magnitude of

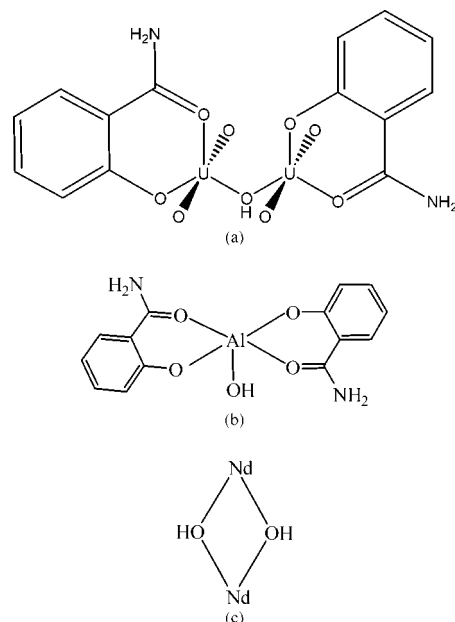


Figure 9. Plausible structures of the complexes $(\text{UO}_2)_2(\text{OH})\text{L}_2^+$ (a), $\text{Al}(\text{OH})\text{L}_2$ (b), and $\text{Nd}_2(\text{OH})_2^{4+}$ (c).

Table 9. Survey of the Formation Constants of the M^{z+} –HL Systems at 25 °C at the Infinite Dilution Reference State

$\log \beta_{pqr}$	UO_2^{2+}	Al^{3+}	Nd^{3+}	Ni^{2+}
$\log \beta_{111}$	-1.1 ± 0.1	-0.6 ± 0.1	-4.5 ± 0.2	-5.8 ± 0.2
$\log \beta_{122}$	-4.2 ± 0.1	-2.8 ± 0.1	-9.6 ± 0.2	/
$\log \beta_{112}$	0.7 ± 0.2	/	/	/
$\log \beta_{121}$	-6.1 ± 0.2	/	/	-14.1 ± 0.2
$\log \beta_{132}$	/	-9.2 ± 0.2	/	/
$\log \beta_{232}$	-5.3 ± 0.2	/	/	/
$\log \beta_{110}$	/	-5.0 ± 0.2	-7.7 ± 0.2	-8.6 ± 0.2
$\log \beta_{120}$	/	-9.1 ± 0.2	/	/
$\log \beta_{220}$	-5.0 ± 0.2	/	-13.4 ± 0.2	/
$\log \beta_{340}$	/	-12.7 ± 0.2	/	/
$\log \beta_{350}$	-14.5 ± 0.2	/	/	/

Table 10. Survey of the Formation Constants, $\log \beta_{pqr}(3\sigma)$, of the M^{z+} –Salicylamide (HL) and of the M^{z+} –Hydrogen–Salicylate (HSal[−]) Systems^a

(pqr)	1 M NaClO_4		1 M NaClO_4		1 M NaClO_4	
	UO_2^{2+}		Nd^{3+}		Ni^{2+}	
	HSal [−]	HL	HSal [−]	HL	HSal [−]	HL
(1, 0, 1)	1.46(6)	1.33(3)				
(1, 1, 1)	$-1.11(1)$	$-1.53(2)$	$-5.97(1)$	$-5.36(2)$	$-6.7(2)$	$-6.31(6)$
(1, 2, 2)	$-4.3(1)$	$-11.17(6)$				
(1, 1, 2)	$0.2_1(1_4)$	$0.29(6)$				
(1, 2, 1)	$-6.45(3)$	$-6.8(2)$	$-14.03(8)$	$-14.8(1)$		
(1, 3, 2)						
(1, 4, 2)						
(2, 3, 2)	$-5.2_7(1_2)$	$-6.0(3)$				

^a For the complexation of UO_2^{2+} and Nd^{3+} ions with HSal^- , see ref 2.

the constants valid at zero ionic strength was evaluated by assuming the validity of SIT.¹⁹ Since the theory is formulated in terms of molal units ($\text{mol} \cdot \text{kg}^{-1}$), constants and other quantities in the following treatment are expressed on the molal scale. The conversion factors were assumed from Grenthe et al.¹¹

According to theory, the activity coefficient, γ_i , of the species i with charge z_i can be expressed in the molal scale at 25 °C in aqueous solution as

$$\log \gamma_i = -z_i^2 D + \sum b(i, k) m_k \quad (8)$$

where $D = 0.51\sqrt{I}/(1 + 1.5\sqrt{I})$ and b is the specific ion interaction coefficient of i with species k of molality m_k . Interaction coefficients are the result of short-range forces and depend on the ionic strength, but the variation in the range $0.5 \leq I \leq 3.5$ molal is sufficiently low that they may be assumed as constants. As a further simplification, interaction coefficients of ions with the same charge type are nearly zero.

Some $b(i, k)$ values, needed for the calculations, have been deduced from various sources. From ref 19, $b(\text{Na}^+, \text{OH}^-) = 0.04$, $b(\text{H}^+, \text{ClO}_4^-) = 0.14$, $b(\text{UO}_2^{2+}, \text{ClO}_4^-) = 0.46$; from ref 20, $b(\text{Na}^+, \text{L}^-) = 0.11$; from ref 2, $b(\text{Nd}^{3+}, \text{ClO}_4^-) = 0.47$; from ref 5, $b(\text{Al}^{3+}, \text{ClO}_4^-) = 0.46$; from ref 17, $b(\text{Ni}^{2+}, \text{ClO}_4^-) = 0.37$; and from ref 11, $b((\text{UO}_2)_2(\text{OH})_2^{2+}, \text{ClO}_4^-) = 0.57$, $b((\text{UO}_2)_3(\text{OH})_5^+, \text{ClO}_4^-) = 0.45$, and $b(\text{Al}_3(\text{OH})_4^{5+}, \text{ClO}_4^-) = 1.30$.

The $b(i, k)$ values for the complexes of stoichiometry (1, 1), (1, 2), (2, 2), (1, 1, 2), (1, 2, 1), (1, 1, 0), and (1, 2, 0) can be estimated on the basis of empirical rules, suggested elsewhere by Ciavatta.²¹

For the complexes $(\text{UO}_2)_2(\text{OH})\text{L}_2^+$, $\text{Al}(\text{OH})\text{L}_2$, and $\text{Nd}_2(\text{OH})_2^{4+}$, the probable specific ion interaction coefficients are deduced from empirical rules derived from plausible structures of the species (Figure 9(a), (b), and (c)).

The short-range interaction of the complexes with medium ions takes place in reduced amounts according to the contact area accessible. From the collected coefficient values, the interaction of the complexes with medium ions, accounting that the coordination of metal cations is six, should be

$$\begin{aligned} b((\text{UO}_2)_2(\text{OH})\text{L}_2^+, \text{NaClO}_4) &= (2.1/6)b(\text{UO}_2^+, \text{ClO}_4^-) + \\ &\quad (2.5)b(\text{Na}^+, \text{L}^-) + (1/2)b(\text{Na}^+, \text{L}^-) = 0.30 \\ b(\text{Al}(\text{OH})\text{L}_2, \text{NaClO}_4) &= (1/6)b(\text{Al}^{3+}, \text{ClO}_4^-) + \\ &\quad (2.5)b(\text{Na}^+, \text{L}^-) + (1/2)b(\text{Na}^+, \text{OH}^-) = 0.20 \\ b(\text{Nd}_2(\text{OH})_2^{4+}, \text{NaClO}_4) &= (2.4/6)b(\text{Nd}^{3+}, \text{ClO}_4^-) + \\ &\quad (2.5)b(\text{Na}^+, \text{OH}^-) = 0.67 \end{aligned}$$

The results of extrapolation are collected in Table 9. The uncertainties assigned to the constants stem primarily from interaction coefficients of complexes, which are estimated as probable within (± 0.05 or ± 0.1) $\text{kg} \cdot \text{mol}^{-1}$.

Discussion

The aim of this work was the comparison of the nature and stability between complexes with the hydrogen-salicylate ion (HSal^-) and salicylamide. For convenience, we have reported in Table 10 the results for UO_2^{2+} , Nd^{3+} , and Ni^{2+} with the two ligands. The complexation of UO_2^{2+} and Nd^{3+} ions with HSal^- has been studied at 25 °C, by potentiometric measurements with a glass electrode, and in 1 M NaClO_4 in a previous work.² The Ni^{2+} - HSal^- system details will be reported in a forthcoming paper.

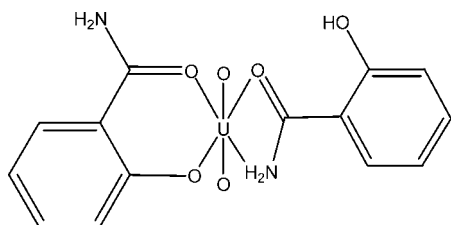
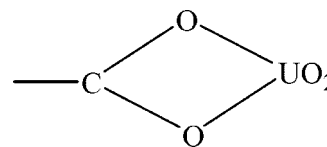


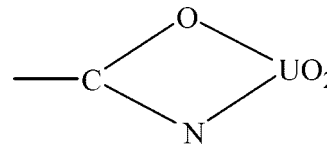
Figure 10. Hypothesis of the structure of the complexes $\text{UO}_2(\text{HL})\text{L}^+$.

The behavior of uranyl toward salicylamide and salicylate ions shows that there are some differences between the two ligands, mainly due to the presence of the species (1, 0, 1) exclusively for the UO_2^{2+} - HSal^- system. However, we cannot exclude the formation of the analogous with salicylamide since it could not be determined by the sensor we have used for these measurements.

In both systems, the species (1, 1, 2) is evidenced. In the salicylate complex, a ligand acts as bidentate, and the other as monodentate through the carboxylate group. Alternatively the ligand HSal^- might be coordinated as bidentate forming a four-term ring.



For the corresponding complex with salicylamide, the structure depicted in Figure 10 can be envisaged in which both ligands act as bidentate.



The formation of the four-term ring presupposes the basic character of the amide group. Some support of this hypothesis stems from constant of equilibrium (5) which become measurable also in water solutions.

A comparison for the aluminum ion can be made between our results and those with hydrogen-salicylate (HSal^-) by Öhman and Sjöberg.²² These authors have found, at 25 °C and in 0.6 M NaCl , the following species: $\text{Al}(\text{Sal})^+$, $\text{Al}(\text{Sal})_2^-$, $\text{Al}(\text{OH})(\text{Sal})_2^{2-}$, and $\text{Al}(\text{OH})_2(\text{Sal})_2^{3-}$. Due to the difference of the ionic strength, the comparison is made on the basis of extrapolated values of the equilibrium constants to the infinite dilution reference state. For the $\text{Al}(\text{III})$ -salicylate species, we found $\log \beta_{111}^\circ = +1.09$, $\log \beta_{122}^\circ = -1.51$, $\log \beta_{132}^\circ = -9.76$, and $\log \beta_{142}^\circ = -20.02$, respectively. The comparison with our results (Table 9) shows that the hydrogen-salicylate ion behaves as a stronger ligand in the most important complexes (1, 1, 1) and (1, 2, 2). On the other hand, the equilibrium constants relative to the minor species (1, 3, 2) seem comparable.

The behavior of neodymium as well as of nickel ions with the two ligands is significantly different. The only common feature is that the main species (1, 1, 1) is always present with comparable stability in all the systems.

In conclusion, salicylamide behaves similarly to salicylate with the uranyl ion only. In all the other systems studied in this work, the differences between the two ligands are more remarkable.

Symbols

HL stands for 2-hydroxybenzamide (salicylamide).

M^{z+} stands for metal cation of charge $z+$.

β_{pqr}° , equilibrium constant for $p\text{M}^{z+} + r\text{HL} \rightleftharpoons (\text{M})^p\text{H}_{-q}(\text{HL})_r^{(z-p-q)+}$.

C_M , C_L , C_B , and C_A stand for molarity ($\text{mol} \cdot \text{dm}^{-3}$) of the metal cation, salicylamide, NaOH , and HClO_4 , respectively.

$Z_H = ([H_3O^+] - K_w[H_3O^+]^{-1} - C_A + C_B)/C_L$ represents the average number of released protons per ligand.

I is ionic strength.

$b(i,k)$ is interaction coefficient between species "i" and "k".

γ_i is activity coefficient of species i on the molal scale.

$[i]$ is molar concentration of species i .

Literature Cited

- (1) Pettit, G. *IUPAC: Stability Constant Data Base*; Academic software: Otley, U.K., 1995.
- (2) Furia, E.; Porto, R. The hydrogen salicylate ion as ligand. Complex formation equilibria with dioxouranium (VI), neodymium (III) and lead (II). *Ann. Chim. (Rome)* **2004**, *94*, 795–804.
- (3) Biedermann, G.; Sillén, L. G. Studies on the hydrolysis of metal ions. IV. Liquid junction potentials and constancy of activity factors in $NaClO_4-HClO_4$ ionic medium. *Ark. Kemi* **1953**, *5*, 425–440.
- (4) Furia, E.; Porto, R. The effect of ionic strength on the complexation of copper (II) with salicylate ion. *Ann. Chim. (Rome)* **2002**, *92*, 521–530.
- (5) Ciavatta, L.; Iuliano, M. A potentiometric study of aluminium (III) phosphate complexes. *Ann. Chim. (Rome)* **1996**, *86*, 1–17.
- (6) Biedermann, G.; Ferri, D. On the preparation of metal perchlorate solutions. *Chem. Scr. (Stockholm)* **1972**, *2*, 57–61.
- (7) Forsling, W.; Hietanen, S., III. The hydrolysis of mercury (I) ion, Hg_2^{2+} . *Acta Chem. Scand.* **1952**, *6*, 901–909.
- (8) Brown, A. S. A type of silver chloride electrode suitable for use in dilute solutions. *J. Am. Chem. Soc.* **1934**, *56*, 646–647.
- (9) Baes, C. F.; Mesmer, R. E. *The Hydrolysis of Cations*; A Wiley-Interscience Publication: New York, 1976.
- (10) Gans, P.; Sabatini, A.; Vacca, A. SUPERQUAD: an improved general program for computation of formation constants from potentiometric data. *J. Chem. Soc., Dalton Trans.* **1985**, *6*, 1195–1200.
- (11) Grenthe, I.; Fuger, J.; Konigs, R. J. M.; Lemire, R. J.; Muller, A. B.; Nguyen-Trung Cregu, C.; Wanner, H. *Chemical thermodynamics of Uranium*; Nuclear Energy Agency Data Bank: Issy-les-Moulineaux, France, 2004.
- (12) Rush, M. R.; Johnson, S. J. Hydrolysis of uranium(VI): absorption spectra of chloride and perchlorate solutions. *J. Phys. Chem.* **1963**, *67*, 821–825.
- (13) Brown, P. The hydrolysis of uranium(VI). *Radiochim. Acta* **2002**, *90*, 589–593.
- (14) Aveston, J. Hydrolysis of the aluminium ion: ultracentrifugation and acidity measurements. *J. Chem. Soc.* **1965**, 4438–4443.
- (15) Kubota, H. Properties and Volumetric Determination of Aluminium Ion. *Diss. Abstr., Univ. of Wisconsin* **1956**, *16*, 864.
- (16) Nazarenko, V. A.; Nevskaya, E. M. Spectrophotometric determination of the constants of mononuclear hydrolysis of aluminum ions. *Russ. J. Inorg. Chem.* **1969**, *14*, 1696–1699.
- (17) Gamsjäger, H.; Bugajski, J.; Gajda, T.; Lemire, R. J.; Preis, W. *Chemical thermodynamics of Nickel*, Nuclear Energy Agency Data Bank; Elsevier Science Publishers: Amsterdam, The Netherlands, 2005; Vol. 6.
- (18) Bolzan, J. A.; Jauregui, E. A.; Arvia, A. J. Hydrolytic equilibria of metallic ions, III. The hydrolysis of Ni(II) in $NaClO_4$ solution. *Electrochim. Acta* **1963**, *8*, 841–845.
- (19) Ciavatta, L. The specific interaction theory in evaluating ionic equilibria. *Ann. Chim. (Rome)* **1980**, *70*, 551–567.
- (20) Furia, E.; Porto, R. On the complexation of copper (II) ion with 2-hydroxybenzamide. *Ann. Chim. (Rome)* **2007**, *97*, 187.
- (21) Ciavatta, L. The specific interaction theory in equilibrium analysis. Some empirical rules for estimating interaction coefficients of metal ion complexes. *Ann. Chim. (Rome)* **1990**, *80*, 255–263.
- (22) Öhman, L. O.; Sjöberg, S. Equilibrium and structural studies of silicon (IV) and aluminium (III) in aqueous solution. 8. A potentiometric study of aluminium (III) salicylates and aluminium (III) hydroxo salicylates in 0.6 M NaCl. *Acta Chem. Scand.* **1983**, *A 37*, 875–880.

Received for review February 27, 2008. Accepted October 18, 2008.

JE800142F